Arab J Sci Eng
DOI 10.1007/s13369-016-2257-5

RESEARCH ARTICLE - CIVIL ENGINEERING

Computation of *R* Factor for Steel Moment Frames by Using Conventional and Adaptive Pushover Methods

M. Gerami[1] · A. H. Mashayekhi[1] · N. Siahpolo[2]

Received: 19 November 2014 / Accepted: 27 June 2016

Abstract Response modification factor, R, can be extracted using static pushover method to reduce the time and complication of dynamic analyses. Recently developed modal and adaptive pushover methods account, respectively, for higher mode effects and changes in structure due to gradual damage during analysis. However, previous attempts on extraction of R factor using pushover method have not incorporated these advances and the present study aims to determine the R factor of steel moment frames using advanced methods. Also, previous researches have determined the target push displacement by monitoring the global behavior of structure and ignoring the collapse modes that may occur due to excessive inter-story drifts. As another innovation, the effect of local collapse modes on R factor of studied frames is accounted for by joint consideration of global and inter-story drifts. Five steel moment frames of 4, 7, 10, 15, and 20 stories are subjected to advanced pushover methods using OpenSees software. It is shown that for high-rise structures subjected to adaptive pushover methods, selection of the response spectrum has a large effect on the resulting R factor. Linear equations are also derived to predict R and other seismic parameters as a function of height and period of structures.

Keywords R factor · Adaptive nonlinear static analysis · Overstrength · Lateral load pattern

✉ N. Siahpolo
n_siahpolo@yahoo.com

1 Earthquake Engineering Group, Faculty of Civil Engineering, Semnan University, Semnan, Iran

2 Department of Civil Engineering, Academic Center for Education, Culture and Research, Khuzestan Branch, Ahwaz, Iran

Published online: 13 July 2016

1 Introduction

Response of structural systems under seismic events is dominated by nonlinear behavior. However, numerical evaluation of this response for each designed structure with account of nonlinearity is avoided by the current guidelines due to its complication and computation cost. These guidelines (e.g., [1,2]) mandate an equivalent procedure for design of regular structures which relies on a linear elastic analysis which is performed under a constant lateral load pattern. Despite the efficiency provided by employment of static load pattern and linear analysis type, the neglect of nonlinearity by the equivalent elastic method leads to errors whose values differ from member to member. Direct account of these errors is not possible due to the simplifications made to the equivalent elastic method. Therefore, assuming to have the capability to provide adequate safety, this method will result in overly strong areas from which the economy of design will suffer. Also, the structural safety provided by this method will not distribute uniformly throughout the structure and the harmony between structural members under extreme conditions is low.

Today, acknowledging some of the mentioned ignorance has become possible with the aid of powerful computers which have revolutionized the engineering problems. In other words, obtaining a more uniform propagation of safety and reducing some level of conservatism has become possible by utilizing more precise methods that represent the ground motion effects more explicitly and with fewer simplifying assumptions.

Elastic design of structures under equivalent lateral loading relies on a predefined constant load pattern along with a number of parameters that account for the nonlinearity of structural behavior through a simple and conceptual presumption. This assumption, which is illustrated in Fig. 1, addresses the relationship between linear and nonlinear

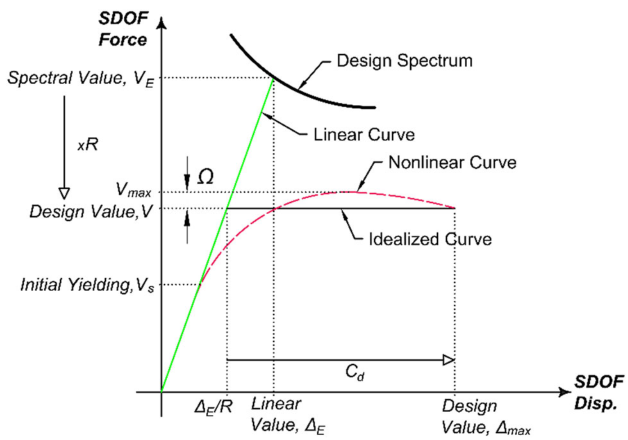

Fig. 1 Equivalent lateral load design concept originated from a SDOF system

response of a single degree of freedom (SDOF) system: the idealized yielding force demand in the real nonlinear structure is computed by scaling down the linear spectral value using a scalar, R, which is called response modification factor. The second parameter used in this regard is ductility, μ, which correlates the actual (nonlinear) value of the maximum deformation demand, $\Delta_{\max}$, to its yielding value. The yielding deformation itself is related to the elastic deformation, Δ_{e}, through the R ratio. Hence, the actual deformation can be approximated as $\Delta_{\max} = \mu \times \Delta_{e}/R$. The ductility ratio is commonly addressed by design standards as deformation amplification factor, C_{d} (Fig. 1). In addition to the R and C_{d} parameters, the ratio between the maximum strength provided by the SDOF system, $V_{\max}$, and the design force, V, is defined as overstrength ratio and is shown by Ω.

For real multiple degrees of freedom (MDOF) structures, R and C_{d} parameters can deliver a meaning after selecting specific force and deformation parameters (commonly the base shear and the roof displacement of a structural frame) that can rationally represent the key structural behavior. Following selecting the key response parameters, the MDOF response can be reduced into a SDOF in which R and C_{d} parameters are the ratios of the precise nonlinear response to the approximate linear estimation. The procedure of representing a MDOF behavior through a SDOF one is illustrated in Fig. 2.

In deriving the codified design methods addressing a specific structural system, both linear and precise nonlinear (static or dynamic) analyses are performed on a finite number of structures representing various configurations of the system and the R and C_{d} factors are derived for each case and are generalized to all configurations of the system following a conservative approach. As mentioned, R and C_{d} values are commonly extracted in terms of maximum base shear and maximum inter-story drift as the representative response parameters. Incorporating these values, the design base shear is applied on the structure following a predefined distribution pattern and the structural members are designed to withstand the resulting forces. Also, the maximum story drift imposed by this loading is amplified by C_{d} factor and is checked against allowable values. As the design forces of the members are derived by assuming a nonlinear behavior, they must be capable of undergoing inelastic deformation without excessive damage. The adequacy of members' ductility is assured by providing construction details which have been examined in practice as well as by conducting experimental programs.

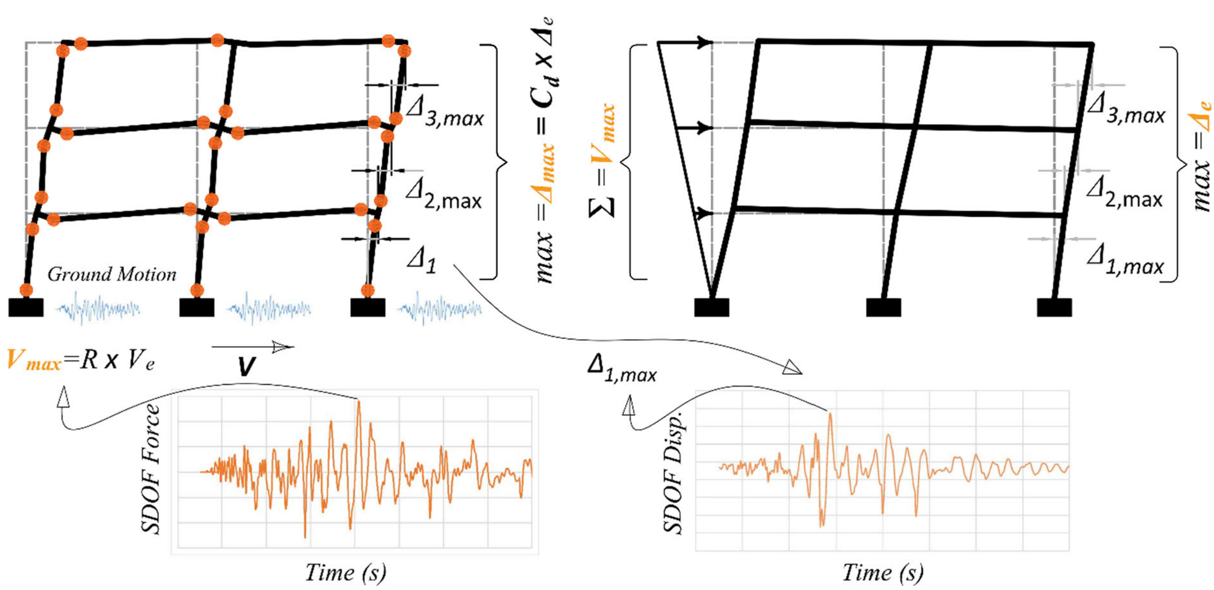

Fig. 2 Using SDOF behavior to summarize the behavior of a MDOF system using representative response parameters

The neglect of nonlinearity in all building degrees of freedom (DOFs) but the ones selected as representative DOFs causes this method to be accompanied by some level of approximation as follows:

(I) Nonlinear deformation of the members is not explicitly addressed and is treated through an empirical approach. The actual deformation of the members which can be directly used for controlling their ductility is neglected. The effect of members' inelasticity on the nonlinear behavior of the structure is not also directly included.

(II) Although the R and C_d parameters are a function of structural configuration such as height, slenderness, degree of indeterminacy, and overstrength content, this correlation is not accounted for.

(III) Distribution of forces and deformations throughout the structure is dependent on the lateral load distribution. While under a real ground motion this distribution is a combination of all building vibration modes, the equivalent lateral load only obeys the first modal shape.

To address these inaccuracies, by keeping the static load pattern, elastic analysis is replaced at the first step by an inelastic analysis which supports for consideration of nonlinearity in multiple freedom degrees of structural behavior. This enhancement leads to nonlinear static, or pushover, method in which the applied loads are gradually increased until a control DOF reaches its predefined target value. After introducing the pushover method, determining target displacements at which state of structural forces and deformations reasonably matches that caused by the design earthquake is the next challenge. Once the pushover analysis is performed up to a suitable target, the R and C_d parameters are not needed any more and the structural nonlinearity can be reflected in the design process through an accurate method. It must be noted that designing the structures using pushover method will involve more propose-evaluate iterations and achieving a converged design solution is more complicated than the equivalent elastic method due to the nonlinearity of the behavior.

To more closely resemble the dynamic effects, two more improvements have been made to conventional pushover analysis (CPA) to evolve it to advanced pushover methods. The first improvement involves multiple, instead of one, modal shapes in the lateral load pattern applied in CPA, and the second updates the modal shapes during the analysis according to the gradual inelasticity formation and the changes in structure's stiffness matrix. These improvements have led, respectively, to modal pushover analysis (MPA) and adaptive pushover analysis (APA) methods.

MPA was introduced by Moghadam and Tso [3] and later by Chopra and Goel [4]. According to MPA, different load patterns corresponding to various elastic mode shapes are applied on the structure until a certain target displacement is reached. The structural responses obtained for each mode are, then, combined using square root of sum of the squares (SRSS) or complete quadratic combination (CQC) methods. The independent application of the load patterns corresponding to different modal shapes makes the interaction between modes to be neglected in the MPA method.

Regarding the APA, two approaches are proposed by Pinho [5] for updating the lateral load pattern following the plasticity change of structure. The force-based adaptive pushover analysis (FAPA) considers the distribution of base shear along structure height to update the load pattern. Displacement-based adaptive pushover analysis (DAPA), on the other hand, uses the distribution of displacement throughout the height for updating the distribution of the lateral load. However, neither of these methods is able to account for the interaction of the vibration modes as was the case of MPA method. To address this inaccuracy, Aydinoğlu [6] proposed the adaptive pushover analysis considering mode interaction (APAM) method based on effective modal masses. APAM considers signs and changes in the characteristics of the structural modal properties caused by plastic hinge formation and stiffness deterioration. APAM estimates the capacity curve using the concept of energy [6].

Although static pushover analysis can be directly used for estimation of seismic force and deformation demands required in a design problem, it has been frequently used as a method for extracting R and C_d parameters related to specific structural systems. These studies are reviewed at the following and have used pushover analysis for reducing the time and complication of nonlinear time history analysis required for deriving the most accurate R and C_d values.

Izadinia et al. [7] investigated the effect of pushover analysis on the R value of moment frames. Their results demonstrated that R and overall ductility calculated by different pushover methods can differ. The greatest yield displacement was calculated by DAPA method. Changes in the loading pattern for CPA caused little change in behavior.

Balendra and Huang [8] found that response modification factor, R, decreased as the number of stories increased. For 3-, 6-, and 10-story braced frames, they found that the response modification factor varied from 8.5 to 3.5. Asgarian and Shokrgozar [9] evaluated the overstrength, ductility, and response modification factor of buckling restrained braced frames of various stories and bracing configurations. They performed static pushover analysis, nonlinear incremental dynamic analysis (IDA), and linear dynamic analysis and found that overstrength, ductility, and response modification factors decreased as the number of stories increased. Kim et al. [10] studied the R of steel concentrically braced frames using IDA and static pushover analysis. The results demonstrated that the factor calculated by IDA is almost identical to the one calculated by pushover analysis and that both values decreased as the number of stories increased. Louzai et al. [11] studied the behavior factor of concrete moment frames using IDA and pushover analysis and found that the R obtained by pushover analysis decreased as the number of stories increased. Kang et al. [12] introduced a method for calculating the behavior factor of steel moment frames. Their results showed that this factor depends on parameters such as design base shear, structural system, failure mechanism, and number of stories.

A study was performed by Attia and Irheem [13] on overstrength, ductility, and response modification factor of X-braced steel frames with different support types, column strong axis orientations, and bay and story numbers. They found that the support type and column orientation parameters changed the R value of structures in the 4.37–10.97 range. The effect of other parameters was minor. In another study, Abdollahzadeh and Abbasi [14] assessed the response modification factor of suspended zipper bracing systems using IDA analysis. The values of 9.5 and 13.6 were recommended for R factors used in ultimate limit state and allowable stress design methods, respectively. Abdi et al. [15] proposed the response modification factors for steel structures equipped with viscous damper devices using static pushover analysis. Damper devices were installed in different locations and various story levels. Results revealed that the response modification factors for steel structures with damper devices are higher than those without damper devices. An equation was proposed to predict the response modification factor for steel structures with viscous dampers having different damping coefficients.

A review of key studies conducted on seismic parameters of steel moment frames in recent years found that the focus of such studies is IDA and conventional pushover analysis with a constant load pattern. Modal and adaptive pushover methods which offer great advances to conventional methods are not used for this purpose. This study, therefore, investigates application of new adaptive and modal pushover methods in estimation of R factor of steel moment frames. For this purpose, pushover analyses have been performed using conventional methods with different lateral load patterns (spectral, first mode, uniform, and triangular) as well as adaptive displacement-based method (DAPA) and adaptive method considering mode interaction (APAM). For extracting the R factor, the newer procedure proposed by FEMA P695 [16] has been utilized instead of the Young approach used in most previous studies [7,17]. The various results obtained using different pushover methods were comparatively assessed, and the effect of (I) various pushover methods and (II) different lateral load pattern types were evaluated. Using the newest pushover methods are the features of the current study against similar studies conducted previously. Another novelty of the present study is consideration of local failure modes in addition to the global instability condition for determining the target displacement. In conventional pushover analyses, the global drift of structure is regarded for detecting the final limit state. The inter-story drifts that may lead to structural collapse before reaching the target roof drift are often ignored. Joint consideration of local and global drifts is regarded in this study for detecting the target displacement. Provision of simple relationships to predict seismic parameters as function of buildings natural periods and heights is another highlight of this study. All pushover analyses have been done using OpenSees [18] software. The structural models were validated against the results obtained by a trusted study before subjecting to the pushover analysis. The OpenSees software is incapable of directing pushover analysis, and thus, codes were provided to perform the analyses.

2 Method for Extracting *R* Parameter

For extracting seismic performance factors, the definitions given in ASCE/SEI 7-05 [1] and illustrated in Sect. 1 and Fig. 1 are regarded. Nonlinear static analysis (pushover) is also conducted following the commentary of the *NEHRP Recommended Provisions* [19]. Response modification factor R (strength reduction factor), system overstrength factor Ω, and deflection modification coefficient C_d values are specified in Table 12.2-1 of ASCE/SEI 7-05 [1] for currently approved seismic-force-resisting systems.

As mentioned in Sect. 1, the elastic base shear of a structure, V_E, can be reduced down to the base shear prescribed for design V. V_E is the lateral force developed in the lateral resisting system which behaves entirely linearly elastic for the design earthquake ground motion (Fig. 1). In calculations performed in this study, V is assumed to equal the maximum (ultimate) base shear, V_max, so that the resulting R is the ultimate R, R_u as:

$$R_\mathrm{u} = \frac{V_\mathrm{E}}{V_\mathrm{max}} \tag{1}$$

By assuming so, the overstrength ratio Ω is differently defined than what provided in FEMA p695 [16] and Sect. 1 (as V_max/V). In the present study, Ω is determined as the ratio of the strength stored in a structure between the formation of the first plastic hinge, V_s, (Fig. 1) and the total yield point of the structure, $V_\mathrm{max}(=V)$, as:

$$\Omega = \frac{V_\mathrm{max}}{V_\mathrm{s}} \tag{2}$$

In Fig. 1, δ_E/R refers to roof displacement of the system corresponding to design base shear, V, assuming that the system remains essentially elastic. The term δ expresses the yielded roof drift corresponding to the design earthquake ground motion. As shown, deflection amplification factor C_d is a fraction of R ($C_\mathrm{d} < R$) and is defined as:

$$C_d = \frac{\delta}{\delta_\mathrm{E}} R \tag{3}$$

3 Structural Models

To investigate the R factor from various pushover analyses, five 2D models with 4, 7, 10, 15, and 20 stories and 4 spans were used. The stories were 4 m high, and the spans had a width of 5 m. All archetypes had a similar floor layout with typical material properties and gravity loads. The selected frames were intermediate SMRFs. The gravity loads were based on the Iranian loading code. For all models, the equivalent dead and live loads acting uniformly on the frame beams were 3250 and 1250 kgf/m, respectively. Building archetypes were designed in detail to strictly comply with the code requirements laid out in ANSI/AISC 341-05 [20] and in ASCE/SEI 7-05 [1] for strength and seismic designs, respectively. The models were checked against both the equivalent lateral load and modal response spectrum procedures.

The calculated inter-story drift at design force was intensified by C_d. The consequent lateral drift was then compared with the allowable drift specified in ASCE/SEI 7-05. For the 4-story model, the maximum allowable drift was 2.5 %; for the 7-, 10-, 15-, and 20-story models, the drift ratio was limited to 2 %. The seismic loading was determined in accordance with the Iranian seismic design code [21]. The design assumptions included soil type III (class D based on FEMA 356) and a high seismic hazard region. Sections used in the frames included box and I-shape sections for columns and beams, respectively. The sections used for the various structures are listed in Table 1. ST37 steel material with a yield strength of 2400 kgf/cm^2 was assumed for all members. All elements were chosen as compact sections (limited local buckling) assuming sufficient lateral support.

4 Performance Criteria

The target displacement was obtained by multiplying the elastic spectral displacement corresponding to the fundamental period using a series of factors representing the ratio of spectral displacement to the elastic roof displacement, the ratio of the elastic displacement to the inelastic displacement, effects related to the hysteresis model of the structural displacement response, and effects related to P–Δ of the displacement response. The target displacement was determined by the methods proposed in FEMA 356 [22] and ATC40 [23].

As determined in FEMA 356 [22], collapse of structural systems must be identified by simultaneous monitoring of global instability and local failure. Global instability of the system is reflected in the target roof displacement limited to the value described in the previous paragraph. For controlling the local member failure, nodal (hinge) rotation of the members was limited to 0.02 radian which is the lower limit prescribed by the ASCE 7-05 [1] standard for restricting the inter-story drifts at the collapse state. The two global and local failure methods have been regarded for determining the target displacement by terminating the analysis by observing the criterion which occurred sooner. Consideration of the local failure criterion is one of the novelties presented in this article.

To maximize the comparability of the pushover analyses performed by employing acceleration records, the earthquake intensities were scaled so that structural collapse was observed in the buildings following the above criteria (simultaneous consideration of local and global failure modes).

5 Ground Motion Details

To perform the adaptive pushover analyses (DAPA and APAM), the displacement and acceleration response spectra from 3 far-field earthquakes were used; their specifications are listed in Table 2. All applied ground motions downloaded from the PEER NGA database were recorded for soil type III based on the Iranian seismic design code or class D per FEMA 356 soil classification. Seismosignal software [24] was used to develop the elastic response spectra for various earthquakes.

6 Modeling Method and Its Verification

Modeling verification is an important step in each study. This issue becomes critical if the research is numerical and requires a significant database. If the modeling assumptions and assemblage have errors, the results will be inaccurate. To prevent this, the modeling method used for the archetype structures was first verified on the 9-story structure shown in Fig. 3. This building was designed by Brandow and Johnson Associates for the SAC Phase II Project (referred to as SAC9 structure). The building is 45.73 m by 45.73 m in plan and 37.19 m in height with 3.96 m typical floor-to-floor heights. Five bays in each direction of 9.15 m in length were selected. SMRF was applied as the lateral force-resisting system. The interior bays contained simple connections and the exterior bay had moment-resisting connections.

Steel wide-flange sections were used as columns with 345 Mpa yield strength. Pinned connections were used at column bases. The floor system was made of steel wide-flange beams acting in composite interaction with the concrete slab. The ground-level seismic mass was 965 t. The mass of the first, second to eighth, and nine level was 1010, 989, and 1070 t,

Table 1 Structural member sizes for *ISMRFs* archetypes

Story	4-story *SMRF*		7-story *SMRF*		10-story *SMRF*		15-story *SMRF*		20-story *SMRF*	
	Columns	Beams	Columns	Beams	Columns	Beams	Columns	Beams	Columns	Beams
1	Box 40X10	PG 40X15	Box 40X15	PG 40X20	Box 40X20	PG 50X20	Box 50X20	PG 50X20	Box 50X25	PG 60X20
2	Box 40X10	PG 40X15	Box 40X15	PG 40X20	Box 40X20	PG 50X20	Box 50X20	PG 50X20	Box 50X25	PG 60X20
3	Box 30X10	PG 40X10	Box 40X15	PG 40X20	Box 40X20	PG 40X20	Box 50X20	PG 50X20	Box 50X25	PG 60X20
4	Box 30X10	PG 40X10	Box 40X10	PG 40X15	Box 40X15	PG 40X20	Box 50X20	PG 50X20	Box 50X25	PG 60X20
5			Box 30X10	PG 40X15	Box 40X15	PG 40X15	Box 50X20	PG 50X20	Box 50X25	PG 60X20
6			Box 30X10	PG 40X10	Box 40X15	PG 40X15	Box 40X20	PG 50X20	Box 50X25	PG 60X20
7			Box 30X10	PG 40X10	Box 40X10	PG 40X15	Box 40X20	PG 50X20	Box 50X20	PG 60X20
8					Box 40X10	PG 40X15	Box 40X20	PG 40X20	Box 50X20	PG 60X20
9					Box 35X10	PG 40X10	Box 40X20	PG 40X20	Box 50X20	PG 60X20
10					Box 35X10	PG 40X10	Box 40X15	PG 40X20	Box 50X20	PG 60X20
11							Box 40X15	PG 40X20	Box 40X20	PG 50X20
12							Box 40X15	PG 40X20	Box 40X20	PG 50X20
13							Box 40X15	PG 40X20	Box 40X20	PG 50X20
14							Box 40X10	PG 40X10	Box 40X20	PG 50X20
15							Box 40X10	PG 40X10	Box 40X15	PG 50X20
16									Box 40X15	PG 50X20
17									Box 40X15	PG 40X20
18									Box 40X10	PG 40X20
19									Box 40X10	PG 40X20
20									Box 40X10	PG 40X20

For the columns, the first number is the outside dimension in cm and the second one is the thickness in mm
For the beams, the first number is the Web depth in cm, and the second one is the Flange width in cm. For all beams the Flange and Web thickness is assumed as 10 mm

Table 2 Characteristics of far-field record set used in DAPA and APAM

Number	Earthquake name	Date (yy-mm-dd)	Station	R (km)	PGA (g)	PGV/PGA (s)	CAV (m/s)	T_p (s)	T_m (s)
1	Chi-Chi, Taiwan	99-09-20	CHY065	83.43	0.1	0.14	9.88	0.56	0.79
2	Loma Prieta	89-10-18	CDMG58224	72.2	0.24	0.15	27.69	0.32	0.86
3	Loma Prieta	89-10-18	CDMG58223	58.65	0.23	0.11	33.26	0.3	0.53

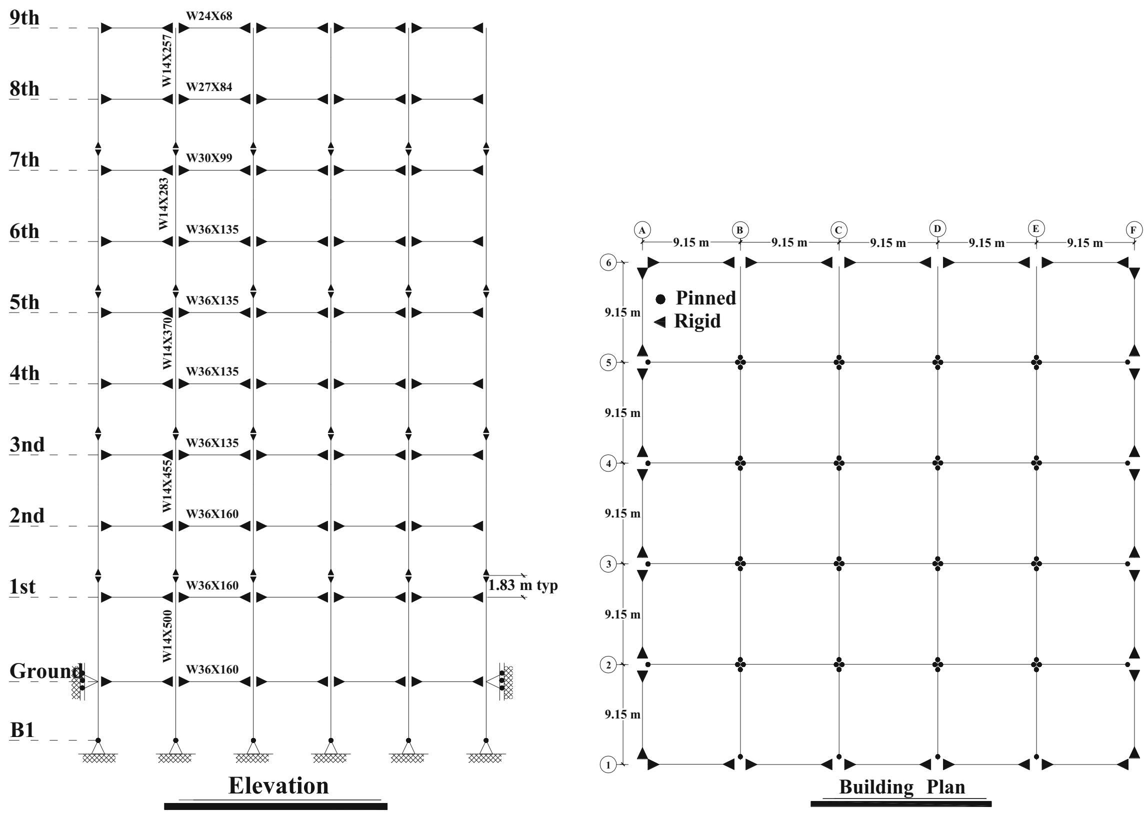

Fig. 3 SAC9 9-story building used for verification of the modeling method (adapted from [25])

respectively. The mass of the entire structure totaled 9000 t. While the SAC9 structure is regular in plan, in the present study, a 2D model consisting of the perimeter N_S SMRF was adopted; thus, half of the seismic mass was assigned to the frame.

The M1 model developed by Gupta and Krawinkler was used [25]. The effect of P–Δ was included, but other effects such as panel zone were neglected. The M1 model is based on a bare frame in which beams and columns extend from centerline to centerline. OpenSees software was used for modeling and analysis of the verification model and archetype structures. The pushover curve resulting from the Gupta study and the 2D model adopted by OpenSees in this study are presented in Fig. 4. A comparison of the graphs approves sufficiency of the modeling method used in this study.

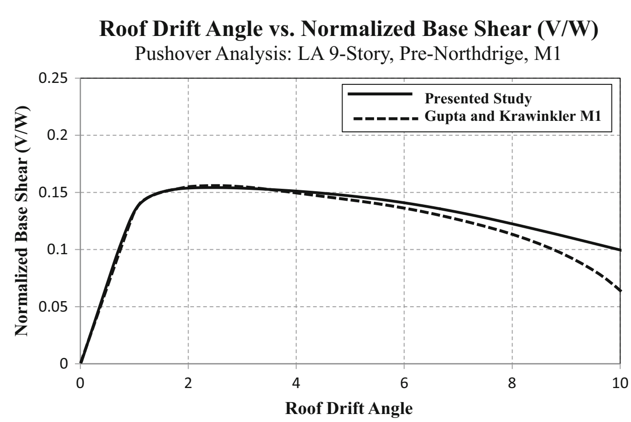

Fig. 4 Pushover curves of SAC9 structure obtained by Gupta and Krawinkler [25,26] and this study

7 Analysis Results

The CPA method with spectral (SPEC), triangular (TR), first mode (M1), and uniform lateral load patterns was applied along with DAPA and APAM methods. In adaptive pushover analyses, the displacement and acceleration response spectra from the three aforementioned far-field earthquakes were used. Figures 5 and 6 show the results of conventional and adaptive NSPs for 7- and 20-story structures. Three types of capacity curves were produced using CPA, DAPA, and APAM.

According to these results, the largest prediction of structural capacity belongs to the uniform pattern of CPA method. The results of the other load patterns used for CPA method are nearly identical. Regarding the adaptive methods, the effect of using different ground motion spectra is minor for the 7-story structure. This effect is, however, more pronounced for the 20-story structure where the adaptive curves obtained using different spectra show larger differences. A comparison between the capacity curves obtained using conventional and adaptive methods also reveals that the difference between the curves increases by increasing the buildings height. This is due to the fact that in taller structures, the higher response modes are more effective than in the shorter ones.

The R factor calculated from various pushover analysis procedures using is presented in Tables 3, 4, 5, 6 and 7 for various structures along with the other parameters. To make the interpretation of the results easier, the minimum R values predicted by each group of methods are selected and shown in Table 8. Similar values are extracted for C_{d} and Ω parameters and are presented in Tables 9 and 10. Figures 7, 8 and 9 depict the values of these tables against height (H) and period (T) of the structures.

As shown in Fig. 7, for all pushover methods, the R values decrease with increase in structures height and period. A similar trend can also be observed for the overstrength factor (Ω) and to a good extent for the deflection amplification factor (C_{d}). These changes can be attributed to the degree of nonlinearity experienced by different structures at the collapse state which is mainly determined by the maximum inter-story drift (0.02). At this deformation level, a lower nonlinearity is experienced by taller buildings which results in a smaller R value.

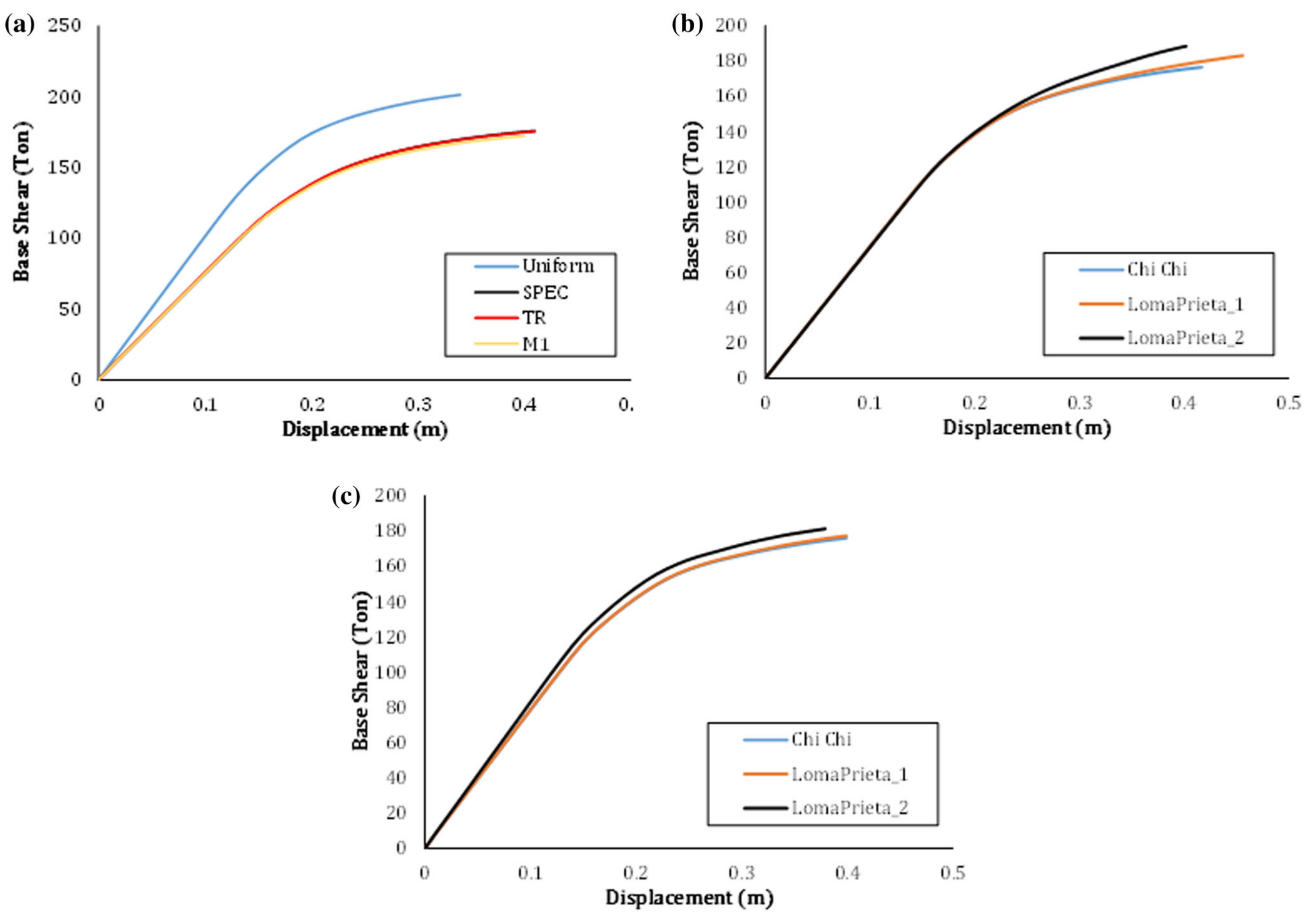

Fig. 5 Pushover/capacity curves for 7-story structure at the collapse state: **a** conventional; **b** DAPA; and **c** APAM

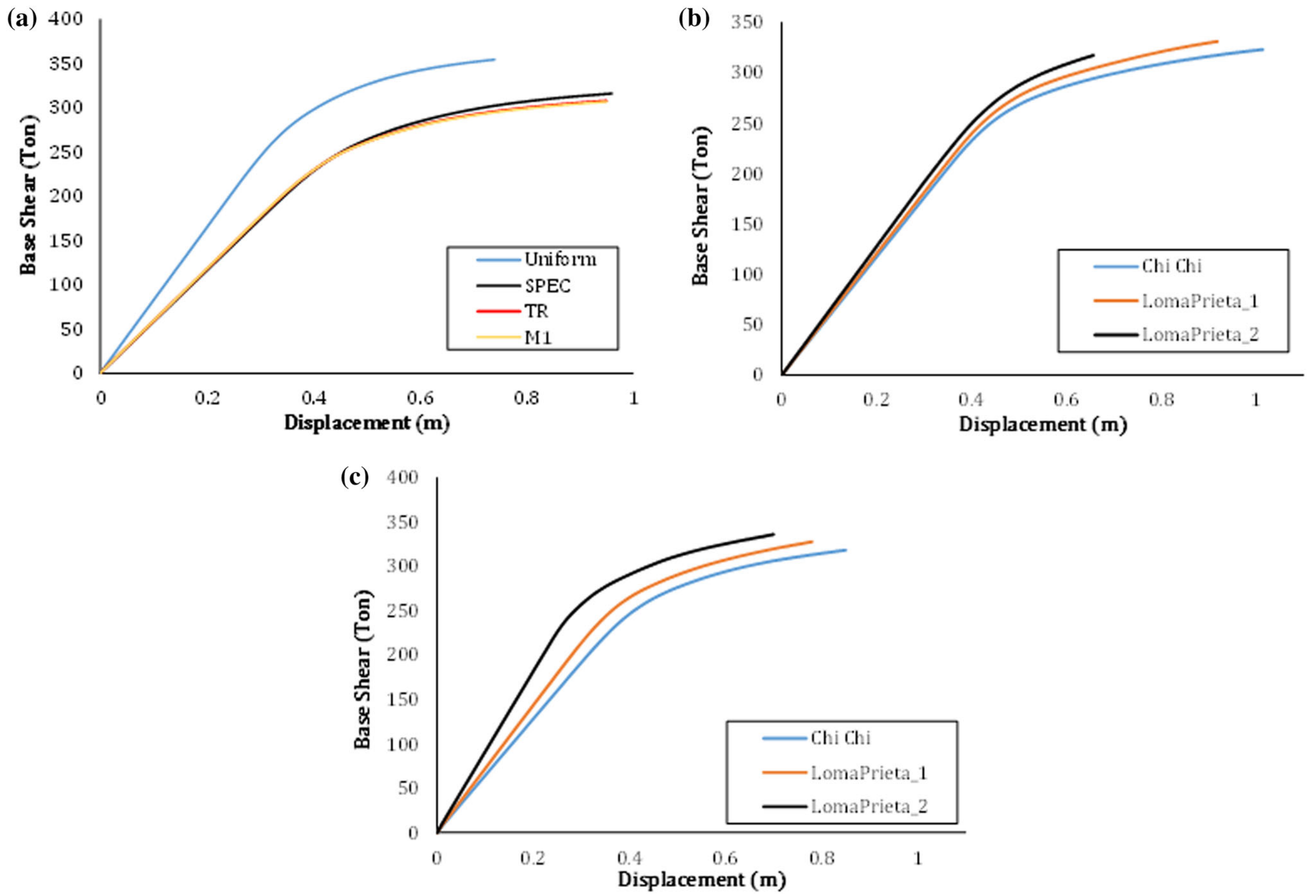

Fig. 6 Pushover/capacity curves for 20-story structure at the collapse state: **a** conventional; **b** DAPA; and **c** APAM

Table 3 Seismic specifications of various NSPs for a 4-story structure

Load pattern IDs	V_s (ton)	V_{max} (ton)	V_E (ton)	Δ_y (m)	Δ_{max} (m)	Ω	C_d	R factor
Uniform	76.73	111.74	1349.8	0.1	0.24	1.46	2.41	12.08
SPEC	60.49	87.25	856.8	0.1	0.25	1.44	2.51	9.82
TR	61.69	89.1	858	0.1	0.24	1.44	2.41	9.63
M1	60.32	87.14	820.9	0.1	0.24	1.44	2.41	9.42
DAP_G1	62.03	91.31	888.4	0.11	0.25	1.47	2.37	9.73
DAP_G2	59.8	91.47	912.9	0.11	0.26	1.53	2.43	9.98
DAP_G3	62.89	92.46	955.1	0.11	0.26	1.47	2.49	10.33
APAM_G1	61.17	88.35	880	0.1	0.25	1.44	2.51	9.96
APAM_G2	61.69	89.06	894.2	0.1	0.25	1.44	2.51	10.04
APAM_G3	63.4	91.6	908.7	0.1	0.24	1.44	2.41	9.92

Also, comparison between the R values estimated by using different pushover methods shows a near similarity at the short stories. For taller buildings, however, different values are resulted from various methods and the R values estimated by the conventional method exceed the other methods. The difference between the conventional and adaptive results elevates with increase in buildings height so that for the 20-story structure a 35 % can be seen. The reason for this increase is again the larger effectiveness of higher response modes in taller buildings which is neglected in conventional method but is accounted for in adaptive methods. The neglect of gradual stiffness loss during conventional pushover analysis can also be responsible for the larger difference in taller buildings. In taller buildings, the secondary moments caused by the P–Δ effects make the structural response more sensitive to stiffness losses.

Table 4 Seismic specifications from various NSPs for a 7-story structure

Load pattern IDs	V_s (ton)	V_{max} (ton)	V_E (ton)	Δ_y (m)	Δ_{max} (m)	Ω	C_d	R factor
Uniform	120.85	168.37	1594.5	0.17	0.34	1.39	2.04	9.47
SPEC	104.39	149.81	1268.9	0.2	0.41	1.44	2.05	8.47
TR	105.15	150.9	1287.2	0.2	0.41	1.44	2.05	8.53
M1	104.39	137.36	1142.8	0.18	0.4	1.32	2.19	8.32
DAP_G1	109.76	142.19	1229.9	0.19	0.42	1.3	2.19	8.65
DAP_G2	115.52	145.79	1385	0.2	0.46	1.26	2.34	9.5
DAP_G3	111.3	141.28	1167	0.19	0.4	1.27	2.12	8.26
APAM_G1	115.9	143.37	1245.9	0.18	0.4	1.24	2.19	8.69
APAM_G2	109.38	143.8	1252.5	0.18	0.4	1.31	2.19	8.71
APAM_G3	114.75	151.47	1313.2	0.18	0.38	1.32	2.08	8.67

Table 5 Seismic specifications from various NSPs for a 10-story structure

Load pattern IDs	V_s (ton)	V_{max} (ton)	V_E (ton)	Δ_y (m)	Δ_{max} (m)	Ω	C_d	R factor
Uniform	147.74	189.73	1457.1	0.22	0.45	1.28	2.08	7.68
SPEC	112.44	157.21	938.5	0.25	0.49	1.4	1.96	5.97
TR	108.52	149.72	898.3	0.23	0.48	1.38	2.06	6
M1	113.1	148.45	841.7	0.23	0.46	1.31	1.97	5.67
DAP_G1	115.71	150.21	929.8	0.24	0.51	1.3	2.11	6.19
DAP_G2	119.63	160.2	1260.8	0.26	0.63	1.34	2.48	7.87
DAP_G3	132.05	167.98	1019.6	0.27	0.5	1.27	1.88	6.07
APAM_G1	119.63	155.55	947.3	0.23	0.47	1.3	2.02	6.09
APAM_G2	124.86	154.38	910.8	0.23	0.46	1.24	1.97	5.9
APAM_G3	137.94	171	1091	0.23	0.45	1.24	1.93	6.38

Table 6 Seismic specifications from various NSPs for a 15-story structure

Load pattern IDs	V_s (ton)	V_{max} (ton)	V_E (ton)	Δ_y (m)	Δ_{max} (m)	Ω	C_d	R factor
Uniform	198.25	253.03	1611.8	0.32	0.66	1.28	2.09	6.37
SPEC	157.36	198.67	1009.2	0.35	0.74	1.26	2.12	5.08
TR	152.41	191.16	955.8	0.33	0.72	1.25	2.16	5
M1	151.17	188.83	919.6	0.33	0.71	1.25	2.13	4.87
DAP_G1	159.84	200.15	1028.8	0.35	0.74	1.25	2.13	5.14
DAP_G2	179.67	219.62	1210.1	0.38	0.78	1.22	2.08	5.51
DAP_G3	178.43	226.45	1268.1	0.38	0.78	1.27	2.05	5.6
APAM_G1	161.08	198.5	911.1	0.32	0.61	1.23	1.93	4.59
APAM_G2	180.91	214.32	1005.1	0.32	0.58	1.18	1.83	4.69
APAM_G3	185.86	216.44	1067	0.3	0.57	1.16	1.9	4.93

Table 7 Seismic specifications from various NSPs for a 20-story structure

Load pattern IDs	V_s (ton)	V_{max} (ton)	V_E (ton)	Δ_y (m)	Δ_{max} (m)	Ω	C_d	R factor
Uniform	237.22	301.7	1611.1	0.37	0.74	1.27	2.02	5.34
SPEC	208.17	270.84	1324.4	0.47	0.96	1.3	2.06	4.89
TR	199.35	264.68	1299.6	0.45	0.95	1.33	2.11	4.91
M1	199.92	255.56	1259.9	0.43	0.95	1.28	2.19	4.93
DAP_G1	212.77	267.16	1399.9	0.46	1.01	1.26	2.23	5.24
DAP_G2	225.99	268.98	1307.2	0.45	0.92	1.19	2.06	4.86
DAP_G3	206.06	252.36	916.1	0.4	0.66	1.22	1.66	3.63
APAM_G1	203.95	266.67	1272	0.42	0.85	1.31	2.04	4.77
APAM_G2	200.31	263.02	1291.4	0.37	0.78	1.31	2.13	4.91
APAM_G3	226.18	272.79	1533.1	0.3	0.7	1.21	2.33	5.62

Table 8 Minimum *R* factor from various NSPs

Pushover methods	4 story	7 story	10 story	15 story	20 story
CPA	9.42	8.32	5.67	4.87	4.89
DAP	9.73	8.26	6.07	5.14	3.63
APAM	9.92	8.67	5.9	4.59	4.77

Table 9 Minimum C_d from various NSPs

Pushover methods	4 story	7 story	10 story	15 story	20 story
CPA	2.41	2.04	1.96	2.09	2.02
DAP	2.37	2.12	1.88	2.05	1.66
APAM	2.41	2.08	1.93	1.83	2.04

Table 10 Minimum Ω from various NSPs

Pushover methods	4 story	7 story	10 story	15 story	20 story
CPA	1.44	1.32	1.28	1.25	1.27
DAP	1.47	1.26	1.27	1.22	1.19
APAM	1.44	1.24	1.24	1.16	1.21

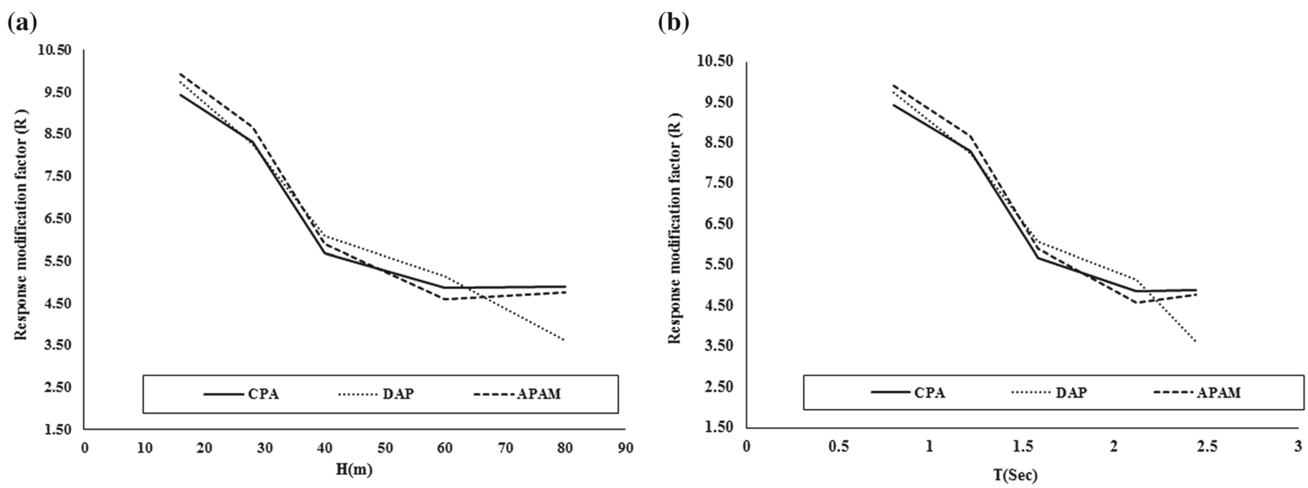

Fig. 7 *R* factor in terms of **a** height and **b** fundamental period

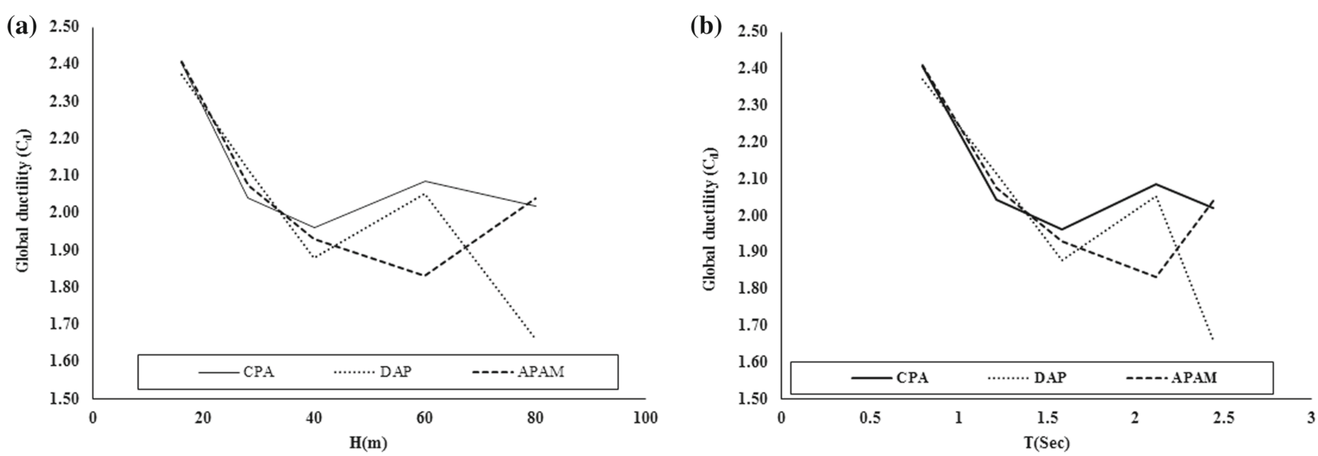

Fig. 8 C_d in terms of **a** height and **b** fundamental period

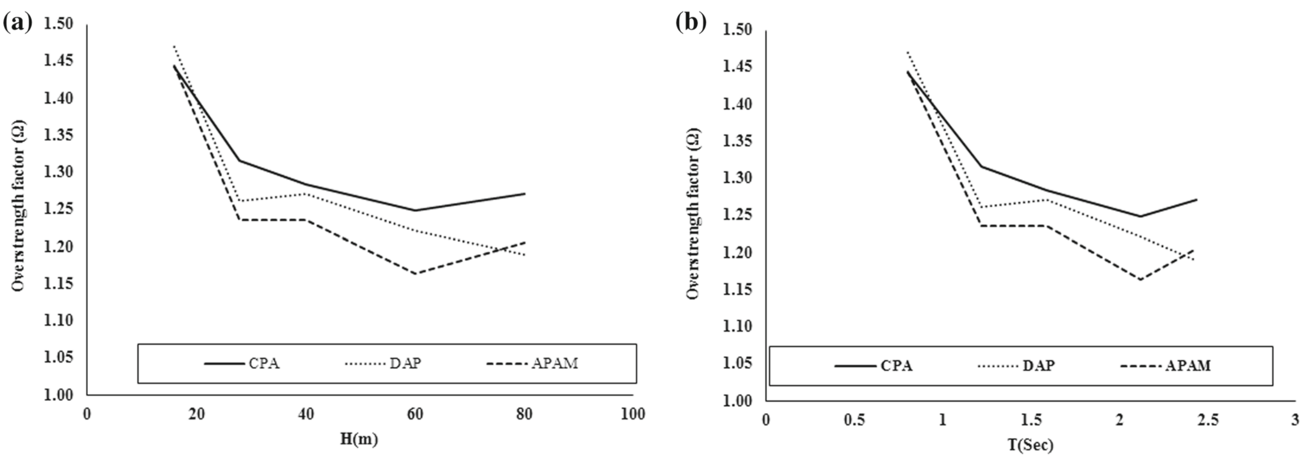

Fig. 9 Ω in terms of **a** height and **b** fundamental period

Table 11 Linear equations for estimating R from different NSPs

Pushover methods	Height (m)	Period (s)
CPA	$R = -0.0738H + 9.94$	$R = -2.9864T + 11.51$
DAP	$R = -0.0931H + 10.74$	$R = -3.634T + 12.50$
APAM	$R = -0.0853H + 10.59$	$R = -3.4452T + 12.40$

Table 12 Linear equations for estimating C_d from different NSPs

Pushover methods	Height (m)	Period (s)
CPA	$C_d = -0.0039H + 2.28$	$C_d = -0.1683T + 2.38$
DAP	$C_d = -0.0089H + 2.41$	$C_d = -0.3404T + 2.57$
APAM	$C_d = -0.0053H + 2.30$	$C_d = -0.2383T + 2.44$

Table 13 Linear equations for estimating Ω from different NSPs

Pushover methods	Height (m)	Period (s)
CPA	$\Omega = -0.0023H + 1.42$	$\Omega = -0.0979T + 1.47$
DAP	$\Omega = -0.0035H + 1.44$	$\Omega = -0.1429T + 1.52$
APAM	$\Omega = -0.0031H + 1.40$	$\Omega = -0.1323T + 1.47$

In order to simplify the application of the results, linear regression equations are derived that correlate R and other seismic parameters to the various parameters affecting them. These equations are presented in Tables 11, 12 and 13 in terms of height (H) and period (T) of the structures.

8 Conclusions

The method presented in FEMA P695 was used to evaluate the seismic design parameters of steel moment frames including overstrength factor (Ω), deflection amplification coefficient (C_d), and response modification factor (R). These parameters were calculated using conventional (CPA) and advanced nonlinear static (pushover) analysis methods. CPA used four lateral load patterns including uniform, triangular, first mode, and the load pattern obtained from spectral dynamic analysis. Advanced pushover analysis included displacement-based adaptive pushover analysis (ADPA) and an adaptive pushover procedure based on effective modal mass combination rule (APAM). All nonlinear analyses were done in OpenSees software. The following results were obtained:

- Response modification factor (R) and overstrength factor (Ω) for all pushover methods decreased as natural period and the number of stories increased.
- R values obtained using a uniform load pattern were larger than the other lateral load patterns used in CPA; thus, using this load pattern in design of structures may lead to un-conservative results.
- R and Ω values obtained using CPA with modal, first mode, and triangular load patterns were almost identical for all structures.
- The type of accelerogram and the nature of records used in DAPA and APAM had an effect on the structural response parameters that elevated with increase in buildings height.
- As the number of stories increased, the difference between R factors obtained by conventional and adaptive pushover analysis increased with a maximum difference of about 35 % for the 20-story structure. This difference was the result of the overly large responses obtained by the CPA. This is mainly caused by the larger effect of the higher modes in high-rise structures which is considered in adaptive analyses.

References

1. ASCE: Minimum design loads for buildings and other structures. American Society of Civil Engineers, Reston (2006)
2. ASCE/SEI7-10: Minimum design loads for buildings and other structures. American Society of Civil Engineers, Reston (2010)
3. Moghadam, A.; Tso, W.: Damage assessment of eccentric multi-story buildings using 3-D pushover analysis. In: Proceedings of Eleventh World Conference on Earthquake Engineering (1996)
4. Chopra, A.K.; Goel, R.K.: A modal pushover analysis procedure for estimating seismic demands for buildings. Earthq. Eng. Struct. Dyn. **31**(3), 561–582 (2002)
5. Pinho, R.; Antoniou, S.: A displacement-based adaptive pushover algorithm for assessment of vertically irregular frames. In: Proceedings of the Fourth European Workshop on the Seismic Behaviour of Irregular and Complex Structures (2005)
6. Abbasnia, R.; Davoudi, A.T.; Maddah, M.M.: An adaptive pushover procedure based on effective modal mass combination rule. Eng. Struct. **52**, 654–666 (2013)
7. Izadinia, M.; Rahgozar, M.A.; Mohammadrezaei, O.: Response modification factor for steel moment-resisting frames by different pushover analysis methods. J. Constr. Steel Res. **79**, 83–90 (2012)
8. Balendra, T.; Huang, X.: Overstrength and ductility factors for steel frames designed according to BS 5950. J. Struct. Eng. **129**(8), 1019–1035 (2003)
9. Asgarian, B.; Shokrgozar, H.: BRBF response modification factor. J. Constr. Steel Res. **65**(2), 290–298 (2009)
10. Kim, J.; Choi, H.: Response modification factors of chevron-braced frames. Eng. Struct. **27**(2), 285–300 (2005)
11. Louzai, A.; Abed, A.: Evaluation of the seismic behavior factor of reinforced concrete frame structures based on comparative analysis between non-linear static pushover and incremental dynamic analyses. Bull. Earthq. Eng. **13**(6), 1773–1793 (2014)
12. Kang, C.-K., Choi, B.-J.: New approach to evaluate the response modification factors for steel moment resisting frames. Int. J. Steel Struct. **11**(3), 275–286 (2011)
13. Attia, W.A.; Irheem, M.M.M.: Boundary condition effect on response modification factor of X-braced steel frames. HBRC J. (2016). doi:10.1016/j.hbrcj.2016.03.002
14. Abdollahzadeh, G.; Abbasi, M.: Response modification factor of suspended zipper braced frames. Steel Compos. Struct. **18**(1), 165–185 (2015)
15. Abdi, H.; et al.: Response modification factor for steel structure equipped with viscous damper device. Int. J. Steel Struct. **15**(3), 605–622 (2015)
16. FEMAP695: P695-Quantification of building seismic performance factors. Federal Emergency Management Agency (FEMA), Document no. 2009, FEMA
17. Uang, C.-M.: Establishing R (or R w) and C d factors for building seismic provisions. J. Struct. Eng. **117**(1), 19–28 (1991)
18. Mazzoni, S.; et al.: OpenSees Command Language Manual. Pacific Earthquake Engineering Research (PEER) Center, Berkeley (2006)
19. Building Seismic Safety Council: NEHRP Recommended Provisions for Seismic Regulations for New Buildings and Other Structures (FEMA 450): Provisions/Prepared by the Building Seismic Safety Council. Building Seismic Safety Council, National Institute of Building Sciences, Washington (2004)
20. ANSI/AISC 341-05: Seismic provisions for structural steel buildings. American Institute of Steel Construction, Chicago (2005)
21. I.S. Code2800: Standard 2800. Building and Housing Research Centre, Tehran (2005)
22. Building Seismic Safety Council: Prestandard and commentary for the seismic rehabilitation of buildings, FEMA-356. Federal Emergency Management Agency, Washington (2000)
23. ATC: Seismic evaluation and retrofit of concrete buildings. Applied Technology Council, report ATC-40. Redwood City (1996)
24. Antoniou, S.; Pinho, R.: Software Seismosignal. 2004, version
25. Gupta, A.; Krawinkler, H.: Seismic Demands for the Performance Evaluation of Steel Moment Resisting Frame Structures. Stanford University, Stanford (1999)
26. Siahpolo, N.; Gerami, M.: Practical Earthquake Engineering, 1st edn. Semnan University, Semnan (2014)